International Journal of Heat and Mass Transfer 125 (2018) 596–603

Contents lists available at ScienceDirect

International Journal of Heat and Mass Transfer

journal homepage: www.elsevier.com/locate/ijhmt

Review

Modularized thermal storage unit of metal foam/paraffin composite

Bofeng Shang [a], Jinyan Hu [a], Run Hu [a], Jingjing Cheng [b,*], Xiaobing Luo [a,*]

[a] State Key Laboratory of Coal Combustion, School of Energy and Power Engineering, Huazhong University of Science and Technology, Wuhan 430074, China
[b] School of Automation, Huazhong University of Science and Technology, Wuhan 430074, China

ARTICLE INFO

Article history:
Received 19 January 2018
Received in revised form 30 March 2018
Accepted 23 April 2018

Keywords:
Modularized thermal storage unit
Metal foams
Paraffin
Effective thermal conductivity
Series-parallel model
Continuous thermal storage

ABSTRACT

Solid–liquid phase change materials (PCMs) are attractive candidates for thermal energy storage and electronics cooling applications, but once all the PCMs have completely phase-changed and approximate their thermal storage limit, they will become the bottleneck for heat dissipation on the contrary and the electronics have to stop working. In this paper, a modularized thermal storage unit (MTSU) was proposed to overcome such fatal drawback. Once the PCMs reach their limit, the completely phase-changed MTSU will be replaced by a new one due to the modularization. Such online thermal charging and offline thermal discharging working characteristics enable the continuous working of electronics. The proposed MTSU is fabricated by encapsulating paraffin with epoxy resin, and the paraffin is thermally enhanced via copper or nickel foams. Theoretical and experimental validations reveal that the ETC is increased by 376% via copper foam with the porosity of 95.52%, and by 205% for nickel foam with the porosity of 95.61% due to the relatively lower skeleton thermal conductivity of nickel foam. The cycled test revealed that the proposed MTSU has good thermal stability. Compared with the conventional TSU, the proposed MTSU avoids the slow re-solidification process and exhibits potential for continuous thermal storage over long periods of time. The proposed MTSU is expected to be applied in the field of driving batteries and solar-thermal conversion system.

© 2018 Published by Elsevier Ltd.

Contents

1. Introduction

Phase-change materials (PCMs) have been applied in thermal energy storage, electronics cooling, and data storage due to its significant latent heat storage capacity [1–8]. However, the real implementation of PCMs is restricted by two main concerns: one is the low intrinsic thermal conductivities which leads to quite slow thermal storage/retrieval process [9–11], and the other is the leakage problem due to the volume expansion in the phase change process [12,13]. In terms of the first concern, efforts have been made to enhance the PCM's thermal conductivity by filling with high thermal conductivity particles or porous matrixes, such as metal powder [14], expanded graphite [15,16], carbon nanotube [17,18], graphene [19,20] and metal foam [21–24]. The PCM thermal conductivity is increased effectively depending on the corresponding filling material and percentage. As for the second concern, the PCMs are usually encapsulated with organic polymers

* Corresponding authors.
E-mail addresses: chengjj@hust.edu.cn (J. Cheng), Luoxb@hust.edu.cn (X. Luo).

https://doi.org/10.1016/j.ijheatmasstransfer.2018.04.117
0017-9310/© 2018 Published by Elsevier Ltd.

to overcome the leakage problem due to the high ductility and high compatibility with PCMs. Huang et al. [25] used PET plastic pipes to encapsulate paraffin and float stones to increase the thermal conductivity, and nearly a third of the melting time can be reduced. Alam et al. [26] adopted polytetrafluoroethylene (PTFE) and fluorinated ethylene propylene (FEP) as shell materials to encapsulate PCM, and the melting/solidification time was significantly shorter without degradation in thermos-physical properties on cycling. More researchers employed epoxy resin as encapsulation material because of its high tensile strength, good adhesive properties, low cost, and high compatibility with PCMs [13,27–29].

However, all these approaches share one significant drawback that once all the PCMs have completely phase-changed, their thermal storage capacity will approximate its maxima and the heat will no longer be stored. More seriously, the PCMs become the key bottleneck for heat dissipation due to their relatively low intrinsic thermal conductivity compared with the metal or semiconductor substrates. The electronic devices have to stop working at that time and wait for the slow re-solidification process of the PCMs before restarting to work [30,31]. Such drawback dramatically restricts the implementation of PCMs for thermal storage applications.

Inspired by the online-discharging/offline-charging working characteristics of the driving batteries [32,33] and the modular thermal energy storage concept [16], we proposed a similar modularized thermal storage unit (MTSU) to overcome such drawback and realize online thermal charging and offline thermal discharging working characteristics. Fig. 1 shows the working principle of the MTSU. During the operating time of electronic devices, the MTSU absorbs the heat from electronics and maintains the designed constant temperature before phase changing totally. Then, the completely charged MTSU could be replaced with a fresh one directly once it reaches the thermal storage limitation. The electronics can continue to work without waiting for the longtime re-solidification process. Therefore, the MTSU can overcome the above-mentioned drawback and enable the continuous working of the electronic devices.

In this paper, we fabricated the MTSU by epoxy resin encapsulated paraffin to validate the online thermal charging and offline thermal discharging working characteristics. Vacuum impregnation and casting molding were adopted to prepare the phase-change core and encapsulate shell, respectively. Paraffin was chosen due to its advantages of high latent heat (~250 J/g), appropriate melting point (30–70 °C), high stability, low negative environmental impact, and low cost. Copper and nickel metal foams with different porosities were employed as thermal enhancers because of high thermal conductivity and good mechanical strength of the skeleton. A series-parallel model was developed to predict the effective thermal conductivity (ETC) of the MTSU samples and the accuracy was verified experimentally. The thermal storage performance of the MTSU was also assessed. The advantages of the proposed MTSU was verified and discussed by comparison with conventional TSU.

2. Preparation of MTSU

Fig. 2 shows the fabrication processes of paraffin/metal foam core through vacuum impregnation [24]. Firstly, the solid paraffin was put in a beaker and melt in a water bath at 80 °C, and the metal foam with a size of 26 mm × 26 mm × 10 mm was immersed in the liquid paraffin. Secondly, the beaker was put into a vacuum oven at 80 °C. The pressure inside the vacuum oven was maintained below 100 Pa for 2 h by a vacuum pump to obtain a desirable impregnation effect in this process. Thirdly, the breaker was cooled at the ambient temperature till the complete solidification. Then, the beaker was reheated in the water bath again. When the inner surfaces of the beaker were wetted by the liquid paraffin, the paraffin/metal foam composite was pulled out. Finally, the extra paraffin outside the metal foam was removed. The thermophysical properties of the paraffin and epoxy resin are listed in Table 1. We can find that both the paraffin and the epoxy resin possess a low thermal conductivity, which demonstrate the necessity of thermal enhancement by metal foam.

The thermally enhanced MTSU was fabricated through casting molding method. Fig. 3 shows the preparation process. Firstly, the epoxy resin (Ausbond®, America) including resin and hardener, were mixed with the mass ratio of 5:1 in a vacuum chamber to expel air bubbles. Secondly, the resin gaskets with a thickness of 2 mm were molded by Mold 1. Thirdly, the paraffin (RT44HC, RUHR TECH®)/metal foam core was put into Mold 2 with the mold-releasing agent (polyvinyl alcohol, PVA) uniformly coated on the surfaces of the molds, and the gaskets were used to retain a fixed distance between the core and mold surfaces. After that, the liquid epoxy resin was injected into Mold 2 to fill the reserved space around the paraffin core. Then, Mold 2 was put into a vacuum chamber to expel air bubbles inside. Finally, the specimen

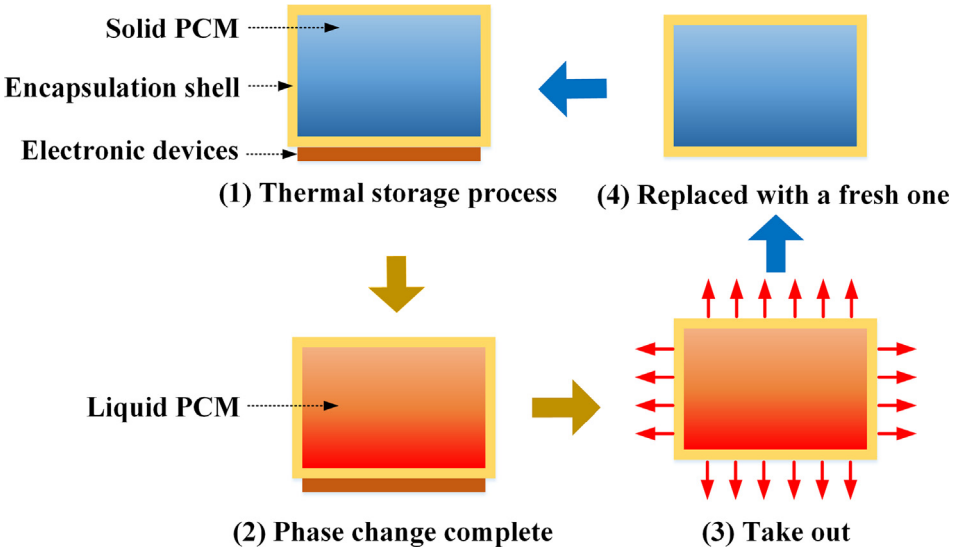

Fig. 1. Working principle of the MTSU samples.

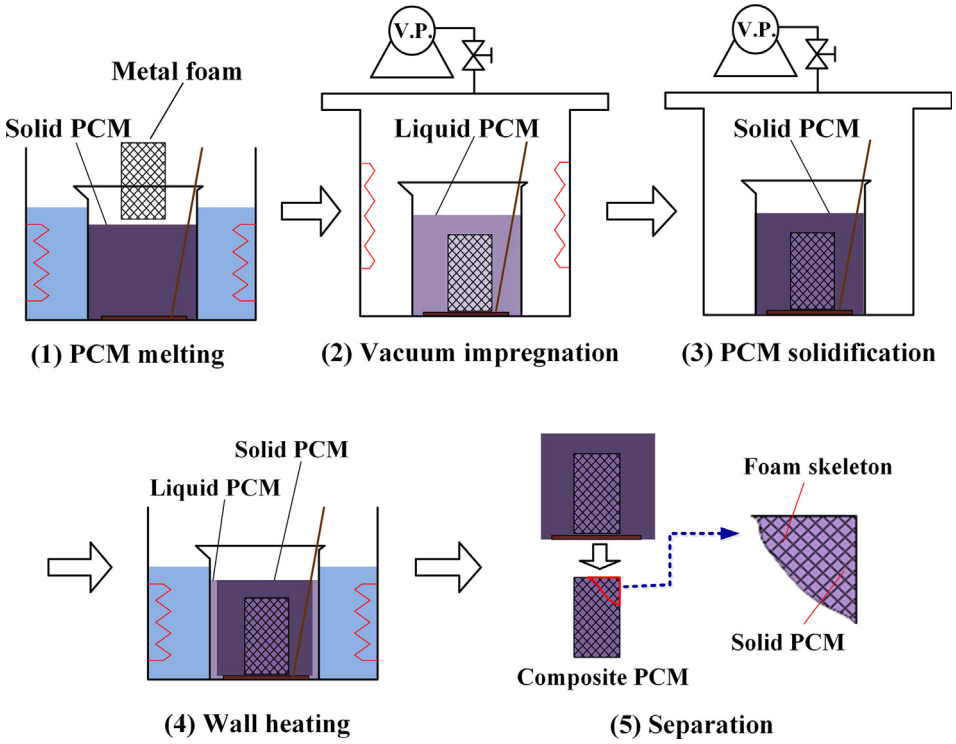

Fig. 2. Vacuum impregnation processes of paraffin/metal foam composite.

Table 1
Thermo-physical properties of paraffin and epoxy resin.

Materials	Density (kg/m^3)	Thermal conductivity (W/m·K)	Latent heat (kJ/kg)
Paraffin	845 (liquid)/860 (solid)	0.2	244
Epoxy resin	1500	0.518	/

was placed in the vacuum chamber for 6 h with curing treatment at 50 °C.

During the preparation process, copper and nickel foams with different porosities were employed to fabricate the thermally enhanced MTSU. The thermo-physical properties of the metal foams are listed in Table 2. Fig. 4a shows the skeletons of the copper foam and nickel foam. It can be seen that the skeleton inside the foam is reticulate and connected layer by layer. Hence, the high

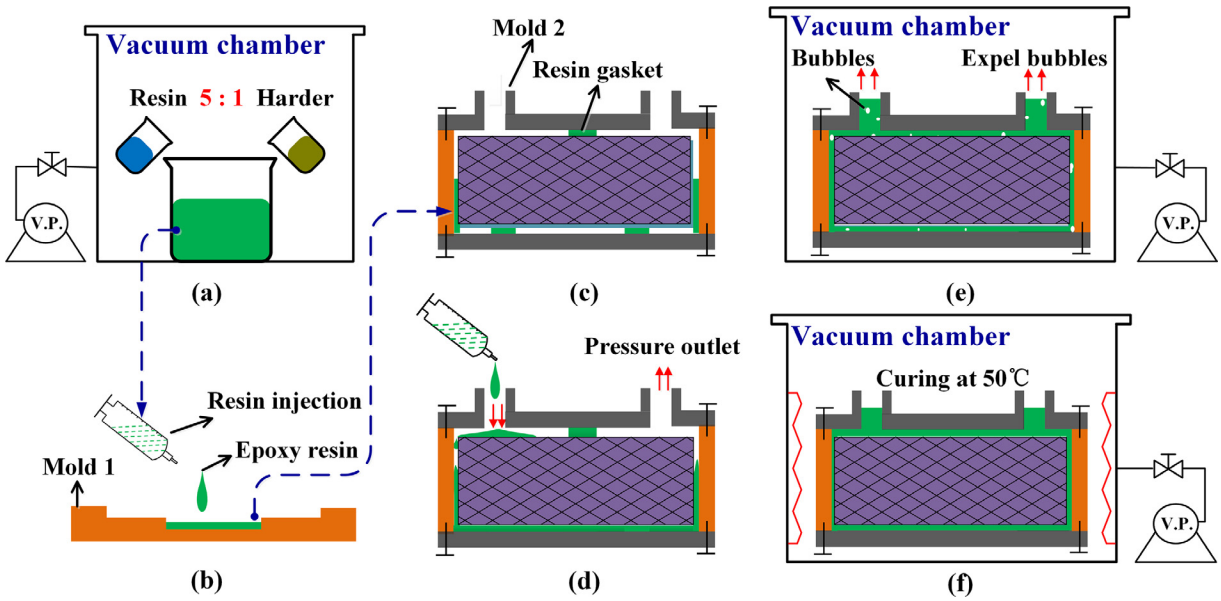

Fig. 3. Preparation processes of the metal foam enhanced MTSU samples.

Table 2
Thermo-physical properties of the metal foams.

Properties	Copper foam		Nickel foam	
	20PPI	30PPI	20PPI	30PPI
Density (kg/m^3)	8930	8930	8900	8900
Thermal conductivity (W/m·K)	398	398	91.4	91.4
Porosity	97.59%	95.52%	97.48%	95.61%

thermal conductivity paths were formed inside the metal foam. Fig. 4b shows the panoramic and cross-sectional view of the MTSU sample. The samples have the dimension of 30 mm × 30 mm × 14 mm, and the thickness of the resin shell is 2 mm.

3. Series-Parallel model

To evaluate the thermal enhancement effect of the metal foams, the ETC of the MTSU was measured. However, common transient thermal conductivity measurement methods were inapplicable due to the anisotropic characteristic of the MTSU [34]. Therefore, we developed a series-parallel model to predict the ETC of the MTSU. Fig. 5 shows the series-parallel model of the MTSU sample, including a series model and a parallel model [35,36]. The MTSU sample could be divided into three layers which formed a series model, then the ETC of the MTSU could be expressed as

$$\lambda_{\text{eff}} = v_1\lambda_1 + v_2\lambda_2 + v_3\lambda_3 \tag{1}$$

where v_1, v_2, and v_3 are the volume fraction of these three layers, respectively. λ_1 and λ_3 are the thermal conductivity of the first and third layer, i.e. the thermal conductivity of the epoxy resin (λ_{er}). λ_2 is the thermal conductivity of the second layer, which consists of the phase change core and the wrap-around resin shell that formed a parallel model, and the expression is as follows.

$$\lambda_2 = \frac{1}{\frac{v_{er2}}{\lambda_{er}} + \frac{v_c}{\lambda_c}} \tag{2}$$

where v_{er2}, and v_c are the volume fraction of resin shell and metal foam/paraffin composite in the second layer, respectively. λ_c is the thermal conductivity of the metal foam/paraffin composite. Then the ETC of the MTSU could be expressed as

$$\lambda_{eff} = \frac{h_1 - h_2}{h_1}\lambda_{er} + \frac{h_2}{h_1}\left(\frac{w_1 l_1 - w_2 l_2}{w_1 l_1 \lambda_{er}} + \frac{w_2 l_2}{w_1 l_1 \lambda_c}\right)^{-1} \tag{3}$$

where h_1 and h_2 are the height of the MTSU sample and the paraffin/metal foam core, respectively. w_1 and l_1 are the width and length of the MTSU sample, while w_2 and l_2 are those of the paraffin/metal foam core. The ETC of the metal foam/paraffin core could be calculated based on the model proposed by Bhattacharya [37] as

$$\lambda_c = \frac{0.75}{\frac{\varepsilon}{\lambda_p} + \frac{1-\varepsilon}{\lambda_m}} + 0.35(\varepsilon \cdot \lambda_p + (1-\varepsilon)\cdot\lambda_m) \tag{4}$$

where ε is the porosity of the metal foam, λ_p is the thermal conductivity of paraffin, and λ_m is the thermal conductivity of metal foam.

4. Experimental validation

The accuracy of the model was evaluated experimentally. Fig. 6a shows the schematic of the experimental setup based on steady-state plate method [38]. Two heat flux sensors were stack on the upper and lower surfaces of the sample. K-type thermocouples were also coupled with the heat flux sensors to measure the average surface temperature. Thermal conductive silicone sheets (TCSS) with a thickness of 0.1 mm were placed in the interfaces between the sample and heat flux sensors, and the thermal conductivity is 1.5 W/(m·K). The cold plate was adopted to remove the heat leakage from the upper heat flux meter and maintain a

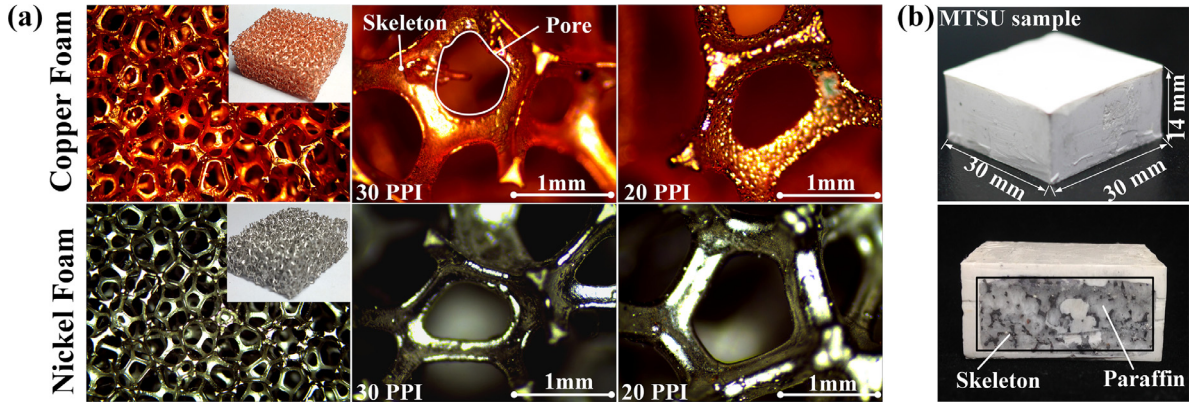

Fig. 4. (a) The skeletons of the copper foam and nickel foam. (b) The MTSU sample.

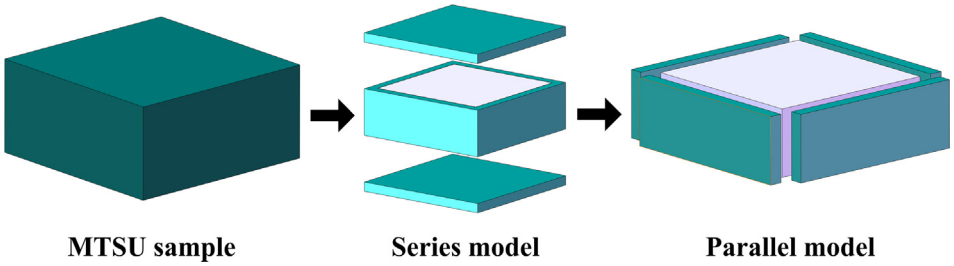

Fig. 5. Series-parallel model of the MTSU sample.

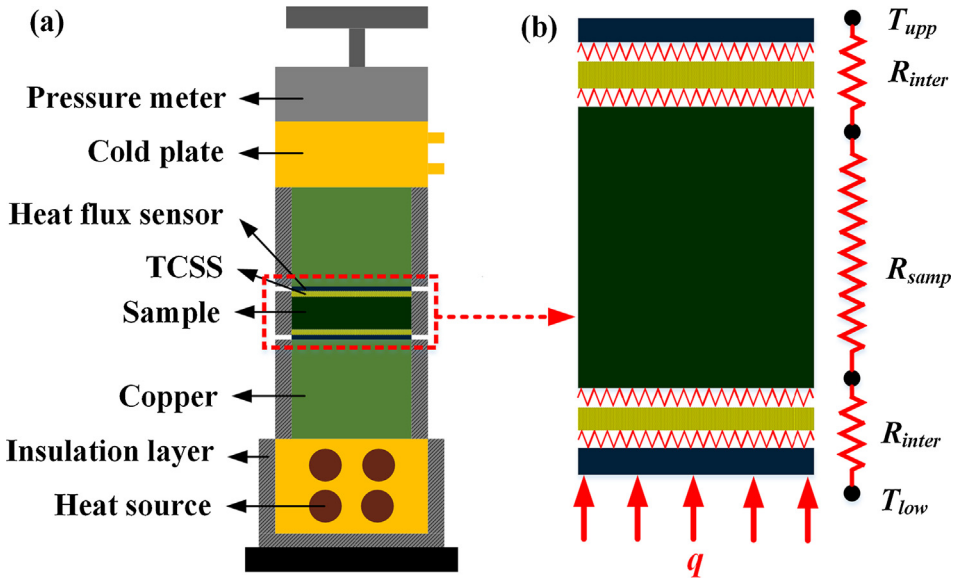

Fig. 6. (a) Schematic of the experimental setup based on steady-state plate method. (b) Thermal resistance model of the test sample.

constant cold temperature. The insulation layer was packed around the copper plate and the samples to eliminate heat leakage to ambient. Consequently, heat flow in flux meter could be regarded as one-dimensional. Fig. 6b shows the thermal resistance model of the test sample. The overall thermal resistance (R_{total}) of the model consists of the bulk thermal resistance of sample (R_{samp}) and two interface thermal resistances (R_{inter}) between the sample and the heat flux sensors, and it could be solved by Eq. (5). The ETC of the MTSU could be calculated by Eq. (6).

$$R_{total} = (T_{low} - T_{upper})/Aq \tag{5}$$

$$\lambda_{eff} = \delta/AR_{total} \tag{6}$$

where T_{low} and T_{upp} are the surface temperature of the lower and upper sensors when the system arrived at the steady state. A is the area of sample and q is the heat flux through the sensors. δ is the thickness of the sample. The R_{inter} consists of the bulk thermal resistance of the TCSS and the thermal contact resistance (TCR) between the TCSS and the sample. R_{inter} was considered to be constant because of the same test conditions. In addition, a pure epoxy resin sample with the same dimension of MTSU was also prepared. The thermal conductivity of the epoxy resin (λ_{er}) was detected to be 0.518 W/m·K, and the thermal resistance of the resin sample could be calculated by Eq. (7). R_{inter} could be solved as Eq. (8). Finally, the ETC of the MTSU (λ_{eff}) could be calculated as Eq. (9).

$$R_{er} = \delta/A\lambda_{er} \tag{7}$$

$$R_{inter} = \frac{1}{2}((T_{low} - T_{upp})/Aq - \delta/A\lambda_{er}) \tag{8}$$

$$\lambda_{eff} = \delta q/(T_{low} - T_{upp} - 2R_{inter}Aq) \tag{9}$$

5. Results and discussion

Table 3 lists the ETC of the samples predicted by the series-parallel model. The MTSU with pure paraffin was also evaluated for comparison and its ETC was 0.302 W/m·K due to the low thermal conductivity of the epoxy resin as well as the paraffin, which cannot meet the demand for a quick thermal response. The ETC was increased by 376% via copper foam with the porosity of 95.52%, revealing a significant thermal conductivity enhancement effect by metal foam. The ETC increased from 1.238 W/m·K to 1.439 W/m·K as the porosities of copper foam decreased from 97.59% to 95.52%. It could be explained that a lower porosity possesses a larger mass fraction of metal foam, which forms a more intensive thermal conductive path, presenting a more significant thermal enhancing effect. The MTSU with nickel foam revealed a similar tendency, and the ETC increased from 0.734 W/m·K to 0.922 W/m·K as the porosities decreased from 97.48% to 95.61%. The thermal enhancing effect of nickel foam is not as desirable as that of the copper foam due to its much lower skeleton thermal conductivity of nickel.

Table 3
ETC of the samples predicted by the series-parallel model.

ETC	MTSU with pure paraffin	Copper foam		Nickel foam	
		20PPI	30PPI	20PPI	30PPI
λ_{eff} (W/m·K)	0.302	1.238	1.439	0.734	0.922
Enhancing ratio	/	310%	376%	143%	205%

Table 4 lists the temperature and the heat flux detected by experiment. It should be noted that the heating power was set below 10 W to maintain a relatively low specimen temperature (below the paraffin melting temperature) to avoid phase change during the experiment. The ETC of the MTSU could be calculated by Eq. (9). The ETC increased from 1.132 W/m·K to 1.524 W/m·K as the porosities of copper foam decreased from 97.59% to 95.52%, while it is increased from 0.753 W/m·K to 0.998 W/m·K for the nickel foam as the porosities decreased from 97.48% to 95.61%. Fig. 7 shows the comparison between model predictions and experimental results. It is observed that the theoretical predictions agree well with the experimental results for both the copper foam and nickel foam enhanced MTSU samples, with the maximum deviation of 9.7%, indicating that the model is appropriate to predict the ETC of MTSU.

Fig. 8 shows the effect of porosity on the ETC of the MTSU. It is seen that the ETC of the copper foam enhanced MTSU could be increased from 0.322 W/m·K to 1.805 W/m·K theoretically while the porosity varies from 1 to 0, while it is increased from 0.322 W/m·K to 1.780 W/m·K for the nickel foam. In addition, it reveals that a significant thermal enhancing effect is achieved as the porosity decreased from 1 to 0.9 due to the thermally conductive

Table 4
The ETC of MTSU measured by experiment.

Detected values	Epoxy resin	MTSU with pure paraffin	Copper foam-enhanced		Nickel foam-enhanced	
			20PPI	30PPI	20PPI	30PPI
T_{low} (°C)	39.3	41.0	36.2	33.4	37.8	34.7
T_{upp} (°C)	8.3	7.9	13.2	14.3	12.1	13.5
q (W/m^2)	1102	698	1707	1856	1305	1401.5
λ_{eff} (W/m·K)	0.518	0.302	1.132	1.524	0.753	0.998

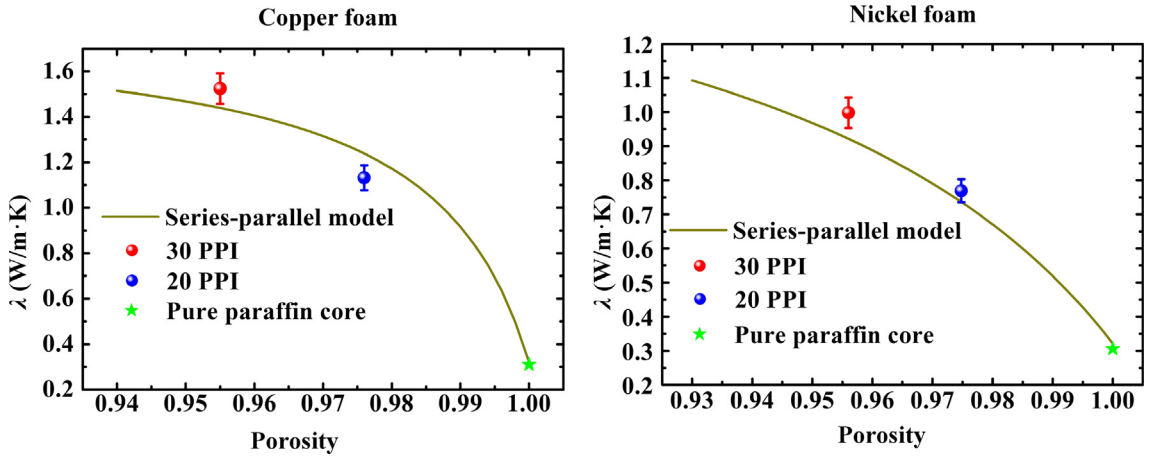

Fig. 7. Comparison of the model predictions with the experimental results.

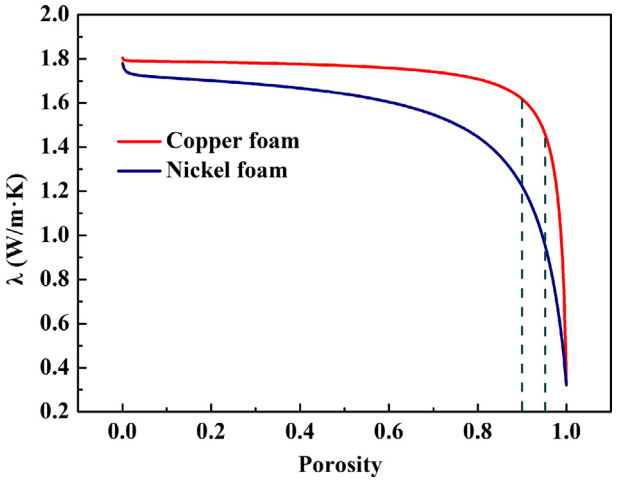

Fig. 8. Effect of porosity on the ETC of the MTSU.

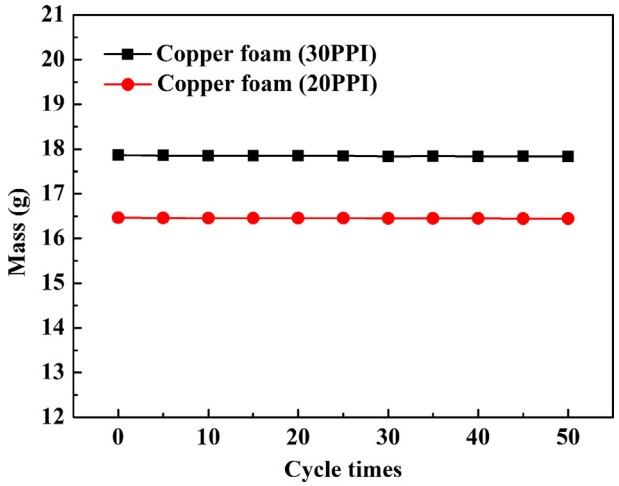

Fig. 9. The mass variation of MTSU with different cycle times.

path formed by metal foam. However, the thermal enhancing effect is not obvious while the porosity is lower than 0.9, which is restricted by the low thermal conductivity of the encapsulation shell, and both the cooper foam and the nickel foam presents the same tendency. In addition, the latent heat of the MTSU decreases with the decreasing porosity accordingly. Therefore, the porosity of the metal foam is preferred to be 0.9–0.95 with comprehensive consideration of the ETC and the latent heat.

The thermal stabilities of the samples were evaluated by the repeated heat storage/release cycles. The tests were conducted in a cycling thermal chamber with the heating temperature of 85 °C and the cooling temperature of 20 °C. The cycle period is 60 min to confirm a completely phase-change of the MTSU samples. Fig. 9 shows the mass variation of the copper foam enhanced MTSU samples with different cycle times. The mass variation is caused by the leakage of paraffin. The thermal stabilities of the samples could be assessed by the mass variation after different cycle times. It observes that the maximum leakage of these two samples were less than 0.2% after 50 cycles, indicating that the MTSU possesses a significant thermal stability performance.

The energy density of the MTSU samples were also evaluated to assess its thermal storage capacity, which mainly dependent on the temperature difference of paraffin. At the temperature difference of 50 °C, the amount of heat production per unit volume for copper foam (30PPI) enhanced MTSU sample is about 175.3 MJ/m^3, revealing a significant thermal storage capacity. The energy density decreased to 155.7 MJ/m^3 at temperature difference of 35 °C. The other samples presented the similar energy density because of the similar amount of paraffin.

To validate the advantage of the proposed MTSU, the heat storage performance of the MTSU was measured experimentally, and the conventional metal foam/paraffin composite phase-change

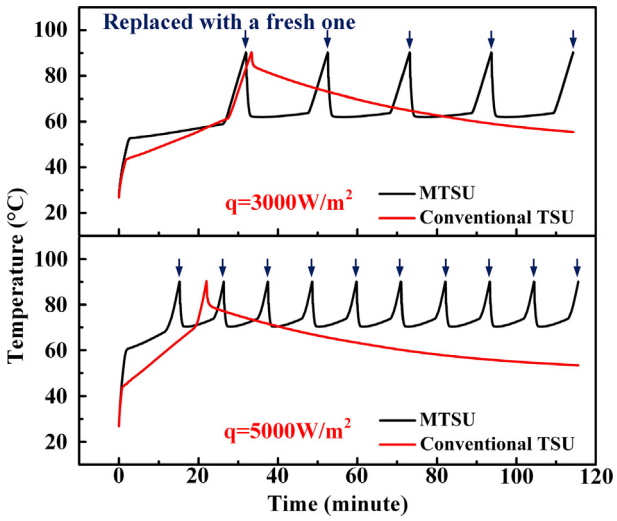

Fig. 10. Comparison of the thermal storage performance between the MTSU and the conventional TSU.

thermal storage unit (TSU) with the same dimension was also tested for contrast. The copper foam (30PPI) enhanced MTSU sample was adopt to exhibit the continuous thermal storage ability compared with the conventional TSU. The design temperature of common electronic devices is usually 90 °C. Fig. 10 shows the comparative results. During the test, the MTSU has replaced a fresh one immediately when the heat source reaches the design temperature, then the heat source temperature decreased rapidly and the online thermal charging and offline thermal discharging working characteristics were reflected. But for the conventional TSU, the heat source has to stop working at that time and wait for re-solidification of the PCMs before restarting to work. It presents an obvious periodic temperature variation process for the MTSU at different heat flux consistently and the heat source temperature was maintained below the design temperature consistently, indicating that the continuous heat storage process was realized. However, the conventional TSU presents a long-time cooling process due to their relatively low thermal conductivity compared with the metal or semiconductor substrates, thus dramatically reducing the working efficiency. Besides, the MTSU seems to show a slower thermal response than the conventional TSU because of the low thermal conductivity encapsulation shell, but the thermal enhancing effect of the metal foam can still guarantee a completely phase-change before the heat source reaches the design temperature. Therefore, the thermal storage performance of MTSU was not affected much. The latent heat of the MTSU was also decreased because of the encapsulation shell, then the single thermal storage time was slightly lower than that of conventional TSU, but the whole thermal storage time was much higher due to the modularization. Besides, the later thermal storage time of the MTSU was lower than that of the first one, because the later MTSU was confronted with a much higher initial heat source temperature, hence the thermal storage time was decreased. In general, the MTSU presents the potential of continuous thermal storage over long periods of time because of the online thermal charging and offline thermal discharging working characteristics.

6. Conclusions

In this study, we proposed a thermally enhanced MTSU to realize the online charging and offline discharging working characteristics. The MTSU samples were fabricated through the vacuum impregnation and the casting molding method. A series-parallel model was developed to predict the ETC of the MTSU samples. An experimental setup based on the steady-state method was also established to verify the accuracy of prediction results. The results showed that the predictions agree well with experimental results and deviations are within 9.7%. Based on the model, we can find that the ETC of the MTSU samples increased drastically with metal foams. The ETC of copper foam-enhanced MTSU increased by 376% while the porosity is 95.52%, and the enhancing effect increases with the decrease of porosity. The repeated heat storage/release cycles revealed that the proposed MTSU possess a good thermal stability. We further evaluated the heat storage performance of the MTSU experimentally. Compared with the conventional TSU, the MTSU avoids the slow re-solidification process and enables a continuous thermal storage process for the electronics, and the electronics temperature was maintained below the design temperature consistently. Therefore, the MTSU shows the potential for continuous heat storage over long periods of time, which is expected to be applied in the field where there is a continuous heat storage demand, such as driving batteries and solar-thermal conversion system.

Conflict of interest

There are no conflicts of interest.

Acknowledgement

The authors would like to acknowledge the financial support by National Natural Science Foundation of China (51625601, 51576078, and 51606074); National Key Research and Development Program of China (2016YFB0100901, 2016YFB0400804); Ministry of Science and Technology of the Peoplés Republic of China (2017YFE0100600).

References

[1] A. Sharma, V.V. Tyagi, C.R. Chen, D. Buddhi, Review on thermal energy storage with phase change material and applications, Renew. Sust. Energy Rev. 13 (2) (2009) 318–345.
[2] B.F. Shang, Y.P. Ma, R. Hu, C. Yuan, J.Y. Hu, X.B. Luo, Passive thermal management system for downhole electronics in harsh thermal environments, Appl. Therm. Eng. 118 (2017) 593–599.
[3] X.B. Luo, R. Hu, S. Liu, K. Wang, Heat and fluid flow in high-power LED packaging and applications, Prog. Energ. Combust. Sci. 56 (2016) 1–32.
[4] G.D. Han, H.S. Li, J.C. Grossman, Optically-controlled long-term storage and release of thermal energy in phase-change materials, Nat. Commun. 8 (1) (2017) 1–10.
[5] R. Hu, H. Zheng, J.Y. Hu, X.B. Luo, Comprehensive study on the transmitted and reflected light through the phosphor layer in light-emitting diode packages, J. Disp. Technol. 9 (6) (2013) 447–452.
[6] Y.P. Ma, R. Hu, X.J. Yu, W.C. Shu, X.B. Luo, A modified bidirectional thermal resistance model for junction and phosphor temperature estimation in phosphor-converted light-emitting diodes, Int. J. Heat Mass Transf. 106 (2017) 1–6.
[7] G. Atwood, Phase-change materials for electronic memories, Science 321 (5886) (2008) 210–211.
[8] F. Xiong, A.D. Liao, D. Estrada, E. Pop, Low-power switching of phase-change materials with carbon nanotube electrodes, Science 332 (6029) (2011) 568–570.
[9] B. Zalba, J.M. Marín, L.F. Cabeza, H. Mehling, Review on thermal energy storage with phase change: materials, heat transfer analysis and applications, Appl. Therm. Eng. 23 (2003) 251–283.
[10] M.K. Rathod, J. Banerjee, Thermal stability of phase change materials used in latent heat energy storage systems: a review, Renew. Sustain. Energy Rev. 18 (2013) 246–258.
[11] R.K. Sharma, P. Ganesan, V.V. Tyagi, H.S.C. Metselaar, S.C. Sandaran, Developments in organic solid–liquid phase change materials and their applications in thermal energy storage, Energy Convers. Manage. 95 (2015) 193–228.
[12] C.Z. Liu, Z.H. Rao, J.T. Zhao, Y.T. Huo, Y.M. Li, Review on nanoencapsulated phase change materials: preparation, characterization and heat transfer enhancement, Nano Energy 13 (2015) 814–826.
[13] W.G. Su, J. Darkwa, G. Kokogiannakis, Review of solid–liquid phase change materials and their encapsulation technologies, Renew. Sust. Energ. Rev. 48 (2015) 373–391.

[14] E.Y. Wang, X.F. Kong, X. Rong, C.Q. Yao, H. Yang, C.Y. Qi, A study on a novel phase change material panel based on tetradecanol/lauric acid/expanded perlite/aluminium powder for building heat storage, Materials 9 (11) (2016) 896.
[15] L. Xia, P. Zhang, R.Z. Wang, Preparation and thermal characterization of expanded graphite/paraffin composite phase change material, Carbon 48 (9) (2010) 2538–2548.
[16] S. Wu, T.X. Li, T. Yan, Y.J Dai, R.Z. Wang, High performance form-stable expanded graphite/stearic acid composite phase change material for modular thermal energy storage, Int. J. Heat Mass Transf. 102 (2016) 733–744.
[17] I. Kholmanov, J. Kim, E. Ou, R.S. Ruoff, L. Shi, Continuous carbon nanotube–ultrathin graphite hybrid foams for increased thermal conductivity and supp0ressed subcooling in composite phase change materials, ACS Nano 9 (12) (2015) 11699–11707.
[18] J.F. Wang, H.Q. Xie, Z. Xin, Thermal properties of paraffin based composites containing multi-walled carbon nanotubes, Thermochim. Acta 488 (1) (2009) 39–42.
[19] H. Babaei, P. Keblinski, J.M. Khodadadi, Thermal conductivity enhancement of paraffins by increasing the alignment of molecules through adding CNT/graphene, Int. J. Heat Mass Transf. 58 (2013) 209–216.
[20] B. Mortazavi, H.L. Yang, F. Mohebbi, G. Cuniberti, T. Rabczuk, Graphene or h-BN paraffin composite structures for the thermal management of Li-ion batteries: a multiscale investigation, Appl. Energy 202 (2017) 323–334.
[21] S. Mancin, A. Diani, L. Doretti, K. Hooman, L. Rossetto, Experimental analysis of phase change phenomenon of paraffin waxes embedded in copper foams, Int. J. Therm. Sci. 90 (2015) 79–89.
[22] W.Q. Li, H. Wan, H.J. Lou, Y.L. Fu, F. Qin, G.Q. He, Enhanced thermal management with microencapsulated phase change material particles infiltrated in cellular metal foam, Energy 127 (2017) 671–679.
[23] W.Q. Li, R.F. Hou, H. Wan, P.J. Liu, G.Q. He, F. Qin, A new strategy for enhanced latent heat energy storage with microencapsulated phase change material saturated in metal foam, Sol. Energy Mat. Sol. C 171 (2017) 197–204.
[24] T.X. Li, D.L. Wu, F. He, R.Z. Wang, Experimental investigation on copper foam/hydrated salt composite phase change material for thermal energy storage, Int. J. Heat Mass Transf. 115 (2017) 148–157.
[25] K.L. Huang, D. Liang, G.H. Feng, M.Z. Jiang, Y.H. Zhu, X. Liu, B. Jiang, Macro-encapsulated pcm cylinder module based on paraffin and float stones, Materials 9 (5) (2016) 361.
[26] T.E. Alam, J.S. Dhau, D.Y. Goswami, E. Stefanakos, Macroencapsulation and characterization of phase change materials for latent heat thermal energy storage systems, Appl. Energy 154 (2015) 92–101.
[27] J.Y. Hu, R. Hu, C. Yuan, B. Duan, M.Y. Huang, X.B. Luo, Fabrication and thermal characterization of the modularized thermal storage unit, IEEE T. Comp. Pack. Man. 6 (8) (2016) 1198–1207.
[28] J.F. Su, Y.H. Zhao, X.Y. Wang, H. Dong, S.B. Wang, Effect of interface debonding on the thermal conductivity of microencapsulated-paraffin filled epoxy matrix composites, Compos. Part A-Appl. S 43 (3) (2012) 325–332.
[29] A.S. Luyt, I. Krupa, Phase change materials formed by uv curable epoxy matrix and fischer–tropsch paraffin wax, Energy Convers. Manage. 50 (1) (2009) 57–61.
[30] M.M. Kenisarin, High-temperature phase change materials for thermal energy storage, Renew. Sust. Energy Rev. 14 (3) (2010) 955–970.
[31] A. Kardam, S.S. Narayanan, N. Bhardwaj, D. Madhwal, P. Shukla, A. Verma, V.K. Jain, Ultrafast thermal charging of inorganic nano-phase change material composites for solar thermal energy storage, RSC Adv. 5 (70) (2015) 56541–56548.
[32] W.Q. Li, Z.G. Qu, Y.L. He, Y.B. Tao, Experimental study of a passive thermal management system for high-powered lithium ion batteries using porous metal foam saturated with phase change materials, J. Power Sources 255 (6) (2014) 9–15.
[33] Z.Y. Ling, F.X. Wang, X.M. Fang, X.N. Gao, Z.G. Zhang, A hybrid thermal management system for lithium ion batteries combining phase change materials with forced-air cooling, Appl. Energy 148 (2015) 403–409.
[34] T. Fiedler, I.V. Belova, G.E. Murch, Critical analysis of the experimental determination of the thermal resistance of metal foams, Int. J. Heat Mass Transf. 55 (2012) 4415–4420.
[35] J.F. Wang, J.K. Carson, M.F. North, D.J. Cleland, A new approach to modelling the effective thermal conductivity of heterogeneous materials, Int. J. Heat Mass Transf. 49 (2006) 3075–3083.
[36] J.F. Wang, J.K. Carson, M.F. North, D.J. Cleland, A new structural model of effective thermal conductivity for heterogeneous materials with co-continuous phases, Int. J. Heat Mass Transf. 51 (2008) 2389–2397.
[37] A. Bhattacharya, V.V. Calmidi, R.L. Mahajan, Thermophysical properties of high porosity metal foams, Int. J. Heat Mass Transf. 45 (2002) 1017–1031.
[38] C. Yuan, B. Duan, L. Li, B.F. Shang, X.B. Luo, An improved model for predicting thermal contact resistance at liquid-solid interface, Int. J. Heat Mass Transf. 80 (2015) 398–406.